FDTD Evaluation of LEMP Considering the Lossy Dispersive Ground

Zheng Sun, Lihua Shi*, Yinghui Zhou, Bo Yang, and Wenwen Jiang

National Key Laboratory on Electromagnetic Environmental Effects and Electro-optical Engineering
PLA Army Engineering University, Nanjing, 210007, China
shilih@tom.com*

Abstract ─ An accurate evaluation of lightning electromagnetic pulse (LEMP) using the finite-difference time-domain (FDTD) method in 2-D cylindrical coordinates is studied, which takes the soil dispersion into account. The parameters of engineering soil models are reformed by the vector-fitting (VF) scheme, for an efficient handling in FDTD. The FDTD updating equations for the dispersive soil are developed with the semi-analytical recursive convolution (SARC) algorithm. The cylindrical CPML is also developed for truncating the dispersive soil. The efficiency of the proposed method is validated by comparing the numerical results with the Cooray-Rubinstein (CR) approximation. The proposed method provides an accurate FDTD evaluation of LEMP considering the soil dispersion and can be further incorporated into the simulations of more complicated LEMP problems.

Index Terms ─ Dispersive soil, FDTD, LEMP, SARC, vector-fitting.

I. INTRODUCTION

The electromagnetic field radiated by the lightning channel is a key threat to the safety of the social electronic equipment, communication systems and power systems. Therefore, it is important to investigate the lightning-radiated electromagnetic field and its propagating property. For the past decades, the precise evaluation of lightning electromagnetic pulse (LEMP) around the lightning channel has drawn worldwide concern. The evaluation methods for LEMP can be divided into three categories: theory, numerical simulations, and experimental validation [1]. Since the analytical formulation is restricted to unrealistically simple configurations and the experiment is not easy to be implemented, the numerical simulation has been increasingly employed in investigations of LEMP problems.

During the past decades, lots of numerical methods, such as the method of moments (MoM) [2], the finite-difference time-domain (FDTD) method [3-5], the finite-element method (FEM) [6,7], the transmission-line-modeling (TLM) method [8], and the partial-element equivalent-circuit (PEEC) method [9], have been adopted to calculate the LEMP generated by return strokes. Among these methods, the FDTD method is the most widespread choice, with the advantages of the efficiently modeling of inhomogeneous parameters, 3-D structures, grounding systems and the complex ground surface.

The FDTD evaluation of LEMP is firstly introduced by Yang [3] in 2-D cylindrical coordinates. And then Baba and Rakov [4] adopted a 3-D FDTD method for the LEMP analysis. Yang [5] proposed a two-step approach for simulating the LEMP problems, by combining the 2-D cylindrical FDTD method and the 3-D FDTD method. For the evaluation of the LEMP radiated from a vertical channel over a rotationally symmetrical ground, it is more advantageous to use the 2-D cylindrical FDTD method, since much less computational resource is required than the 3-D FDTD method.

The ground electronic parameters play an important role in the evaluation of LEMP. For the lightning frequency range, soil materials may exhibit relatively dispersive properties, which can affect the distributions of the LEMP [3, 6, 7]. However, in the FDTD evaluation of LEMP, the ground electronic parameters are always assumed either as a perfect electric conductor (PEC) or as a lossy homogeneous medium characterized by constant electrical parameters. To the best of our knowledge, none of the reports on the FDTD evaluation of LEMP has taken the dispersive property of soil into account.

In this paper, the 2-D cylindrical FDTD method for evaluation the LEMP is developed, which takes the soil dispersion into account. With the vector-fitting scheme [10], the engineering model of the dispersive soil is translated into a new form, which can be easily dealt with in FDTD. The FDTD updating equations for dispersive soil are developed by introducing the semi-analytical recursive convolution (SARC) algorithm [11]. For truncating the dispersive soil, the updating equations of CPML are also developed in cylindrical coordinates. The validation of the proposed method is proved by comparing its numerical results with those obtained from the Cooray-Rubinstein (CR) approximation [12]. The proposed method can be further incorporated into the

Submitted On: November 16, 2016
Accepted On: October 4, 2017

two-step method [5] to simulate more complicated LEMP problems, such as the coupling of underground cables and cavities.

II. METHODOLOGY

A. Computational model

In engineering models, the lightning channel is assumed to be straight and vertical to a rotationally symmetrical ground, as shown in Fig. 1. The field components H_φ, E_ρ, E_z are all independent of azimuth angle, therefore the lightning electromagnetic field around the lightning channel can be simulated by the two-dimensional FDTD in cylindrical coordinates [3]. The 2D-FDTD mesh is also depicted in Fig. 1.

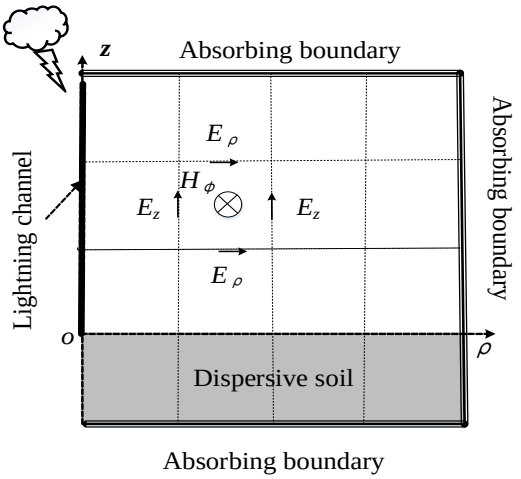

Fig. 1. Computational configurations.

The FDTD evaluation of the LEMP is achieved by solving the Maxwell's equations in the simulation area, with lightning currents along the lightning channel as exciting sources. For an isotropic, inhomogeneous, conductive, linear medium, the Maxwell's equations in the two-dimensional cylindrical coordinates (TMz) can be written as [13]:

$$-\mu_0 \frac{\partial H_\varphi}{\partial t} = \frac{\partial E_\rho}{\partial z} - \frac{\partial E_z}{\partial \rho}, \tag{1a}$$

$$\frac{\partial D_z}{\partial t} + \sigma E_z = \frac{1}{\rho}\frac{\partial (\rho H_\varphi)}{\partial \rho} = \frac{\partial (H_\varphi)}{\partial \rho} + \frac{H_\varphi}{\rho}, \tag{1b}$$

$$-\frac{\partial D_\rho}{\partial t} - \sigma E_\rho = \frac{\partial H_\varphi}{\partial z}, \tag{1c}$$

where μ_0 is the permeability of free space, σ is the conductivity. D_ρ, D_z are the displacement, which satisfy the constitutive relation to the electric field in frequency domain:

$$\begin{aligned} D_s(\omega) &= \varepsilon_0 \varepsilon_r(\omega) E_s(\omega) \\ &= \varepsilon_0 \left(\varepsilon_r'(\omega) - \mathrm{j}\varepsilon_r''(\omega)\right) E_s(\omega) \quad s = \rho, z \end{aligned}, \tag{2}$$

where ε_0 is the permittivity of free space, $\varepsilon_r(\omega)$ is the relative permittivity. $\varepsilon_r'(\omega)$ and $\varepsilon_r''(\omega)$ are the real part and the image part of $\varepsilon_r(\omega)$, respectively. According to the Fourier transform, (2) in time domain can be derived as:

$$D_s(t) = \varepsilon_0 \varepsilon_r(t) * E_s(t), \tag{3}$$

where $*$ is the convolution operator. When $\varepsilon_r(\omega)$ is frequency-dependent, solving the convolution results by direct-integration with FDTD is much time consuming.

B. Parameters of the dispersive soil

(1) Longmire & Smith model

The engineering models for dispersive soils are expressed in terms of curve-fitting expressions for the soil conductivity and relative permittivity based on experimental data. In this paper, we use the universal Longmire & Smith (LS) model [14] to represent the electrical parameters of dispersive soils. Based on the experimental data of Scott, the LS model expresses the soil parameters as functions of frequency and percentage of water content:

$$\sigma_{LS}(f) = \sigma_0 + \sigma_f'(f) = \sigma_0 + 2\pi\varepsilon_0 \sum_{n=1}^{N} \frac{a_n f_n (f/f_n)^2}{1+(f/f_n)^2}, \tag{4a}$$

$$\varepsilon_{r,LS}(f) = \varepsilon_\infty + \varepsilon_f'(f) = \varepsilon_\infty + \sum_{n=1}^{N} \frac{a_n}{1+(f/f_n)^2}, \tag{4b}$$

where $\sigma_0 = 8\cdot(p/10)^{1.54}\cdot 10^{-3}$ is the low-frequency conductivity at 100 Hz, f is the frequency, ranging from DC to 5 MHz, $\sigma_{LS}(f)$ and $\varepsilon_{r,LS}(f)$ are the soil conductivity and relative permittivity at each frequency, respectively. p is the water percentage of soil, and a_n are coefficients presented in Table 1. The LS model satisfies the Kramers–Kronig relationships, and thus provides causal results [15]. Typical curves associated with the frequency dependence of the soil relative permittivity and conductivity for different soil water contents are shown in Fig. 2.

Table 1: Coefficients a_n of the LS model

n	1	2	3	4	5	6	7
a_n	3.4e6	2.74e5	2.58e4	3.38e3	526	133	27.2
n	8	9	10	11	12	13	14
a_n	12.5	4.8	2.17	0.98	0.392	0.173	0

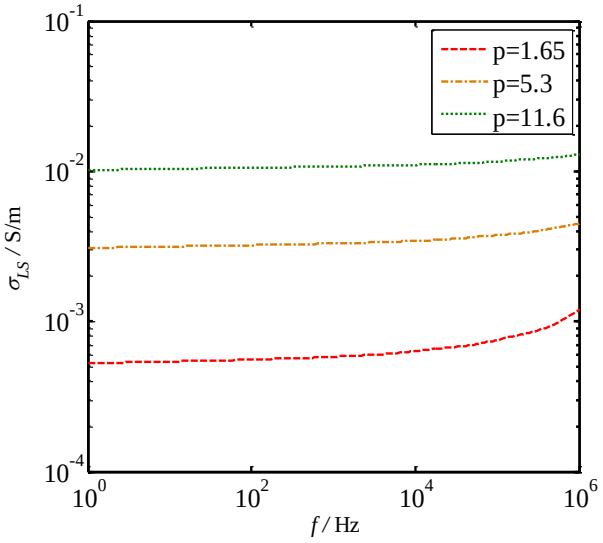

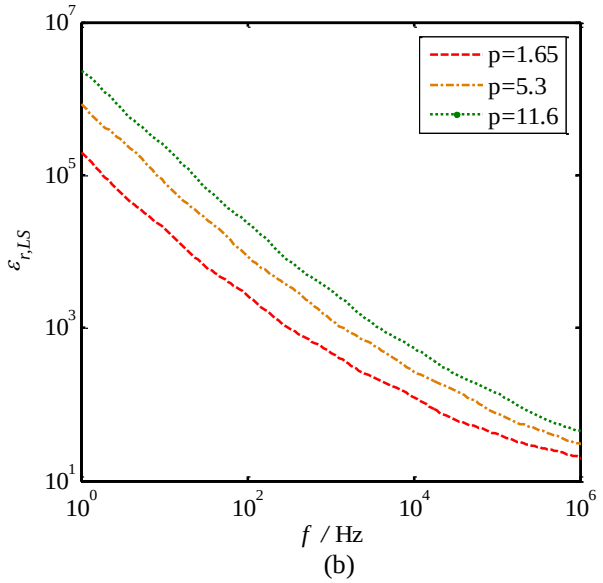

Fig. 2. Parameters of the dispersive soil over the frequency range of interest with different soil water contents: (a) relative permittivity and (b) conductivity.

(2) Translate LS model into FDTD parameters

The relations between the parameters of LS model and those in FDTD are [15]:

$$\sigma_{FDTD} = \sigma_0 , \tag{5a}$$

$$\varepsilon_{r,FDTD}(\omega) = \varepsilon_r'(\omega) - \mathrm{j}\varepsilon_r''(\omega)$$
$$= \varepsilon_{r,LS}(f) + \frac{\sigma_f'(f)}{j2\pi f \varepsilon_0} = \varepsilon_{r,LS}\left(\frac{\omega}{2\pi}\right) + \frac{\sigma_f'(\omega/2\pi)}{j\omega\varepsilon_0} . \tag{5b}$$

The high order rational fraction form of $\varepsilon_{r,FDTD}$ is difficult to deal with in FDTD scheme. Therefore, we employ the vector-fitting scheme [10] to reform $\varepsilon_{r,FDTD}$ as:

$$\varepsilon_{r,FDTD}(\omega) = \varepsilon_c + \chi(\omega) = \varepsilon_c + \sum_{q=1}^{Q} \frac{r_q}{j\omega - p_q} , \tag{6}$$

where ε_c is constant, r_q , p_q are the residues and poles, respectively. The fitting results and the relative fitting errors of the relative permittivity for different water contents are shown in Fig. 3. As we can see, the VF fitting results are excellent. The differences between the curves p=5.3 and p=11.6 caused by the different fitting orders Q employed (Q=17 for p=5.3, Q=14 for p=1.65 and p=11.6).

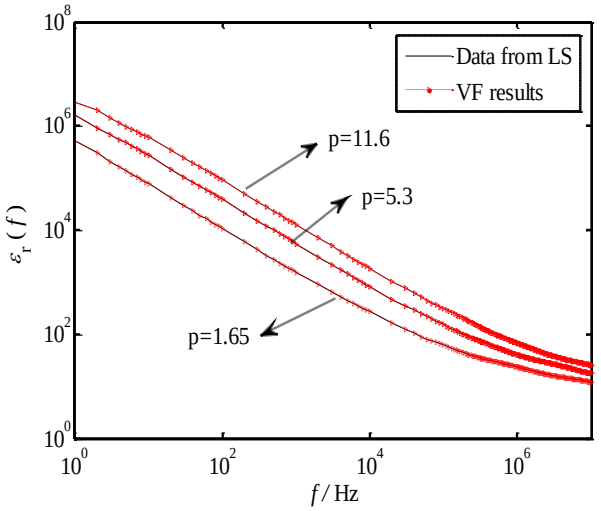

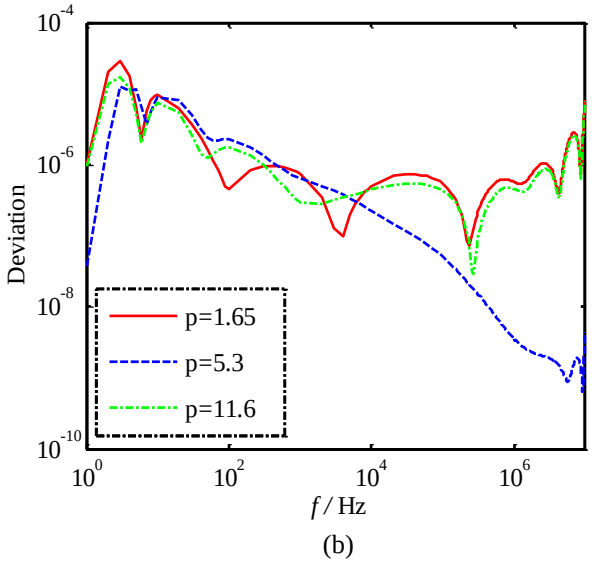

Fig. 3. The vector-fitting results of ε_r with different soil water contents p: (a) VF results and (b) deviations.

C. FDTD Updating equations for the dispersive soil

(1) Algorithms for the constitutive relation [11]

If $\varepsilon_r(\omega)$ has the form of (6), according to the frequency-time relation $1/(\alpha+j\omega)\rightarrow\exp(-\alpha t)U(t)$, the translation form of (2) in time domain is:

$$\begin{aligned} D_s(t) &= \varepsilon_0\left(\varepsilon_c E_s(t)+E_s(t)*\chi(t)\right) \\ &= \varepsilon_0\left(\varepsilon_c E_s(t)+E_s(t)*\left(\sum_{q=1}^{Q} r_q\exp(p_q t)U(t)\right)\right), \\ &= \varepsilon_0\left(\varepsilon_c E_s(t)+\sum_{q=1}^{Q}\psi_{s,q}^{n}(t)\right) \end{aligned} \quad (7)$$

where $$\psi_{s,q}(t)=E_s(t)*r_q\exp(p_q t)U(t). \quad (8)$$

Discretize (8) with time interval $t=n\Delta t$, we obtain:

$$\begin{aligned} \psi_{s,q}^{n} &= \int_0^{n\Delta t} r_q\exp\left(p_q(n\Delta t-\tau)\right)E_s(\tau)\,d\tau \\ &= \int_0^{(n-1)\Delta t} r_q\exp\left(p_q(n\Delta t-\tau)\right)E_s(\tau)\mathrm{d}\tau \\ &\quad +\int_{(n-1)\Delta t}^{n\Delta t} r_q\exp\left(p_q(n\Delta t-\tau)\right)E_s(\tau)\mathrm{d}\tau \\ &= \exp(p_q\Delta t)\cdot\psi_{s,q}^{n-1}+y_{s,q}^{n} \end{aligned}, \quad (9)$$

where

$$y_{s,q}^{n}=r_q\exp(p_q n\Delta t)\cdot\left(\int_{(n-1)\Delta t}^{n\Delta t}\exp(-p_q\tau)\right)E_s(\tau)\,d\tau\Big). \quad (10)$$

If we replace E_s over the time interval $[(n-1)\Delta t, n\Delta t]$ with the average approximation $(E_s^n+E_s^{n+1})/2$, we can get:

$$y_{s,q}^{n}=\exp(-p_q\Delta t)y_{s,q}^{n-1}+c_{0,q}(E_s^n+E_s^{n-1})/2, \quad (11)$$

where

$$c_{0,q}=\begin{cases} r_q\Delta t & p_q=0 \\ -\dfrac{r_q}{p_q}\left(1-\exp(p_q\Delta t)\right) & p_q\neq 0 \end{cases}. \quad (12)$$

(2) FDTD updating equations for the dispersive soil

Discretize (1c) with FDTD method [13]:

$$\begin{aligned} &-\frac{D_{\rho\,i+1/2,j}^{n+1}-D_{\rho i+1/2,j}^{n}}{\Delta t}-\sigma\frac{E_{\rho\,i+1/2,j}^{n+1}+E_{\rho i+1/2,j}^{n}}{2} \\ &=\frac{H_{\varphi\,i+1/2,j+1/2}^{n+1/2}-H_{\varphi\,i+1/2,j-1/2}^{n+1/2}}{\Delta z} \end{aligned}. \quad (13)$$

Substitute (7) into (13), we obtain the updating equation for E_ρ:

$$\begin{aligned} E_{\rho\,i+1/2,j}^{n+1} &= CA\cdot E_{\rho i+1/2,j}^{n} \\ &-CB\cdot\Delta t\cdot\frac{H_{\varphi\,i+1/2,j+1/2}^{n+1/2}-H_{\varphi\,i+1/2,j-1/2}^{n+1/2}}{\Delta z}, \\ &+CB\cdot\varepsilon_0\cdot\sum_{q=1}^{Q}\left((1-\exp(p_q\Delta t))\psi_{\rho,qi+1/2,j}^{n}\right) \end{aligned} \quad (14)$$

where

$$CA=\frac{\varepsilon_0(\varepsilon_c-\frac{1}{2}\sum_{q=1}^{Q}c_{0,q})-\frac{\sigma\Delta t}{2}}{\varepsilon_0(\varepsilon_c+\frac{1}{2}\sum_{q=1}^{Q}c_{0,q})+\frac{\sigma\Delta t}{2}}, \quad (15a)$$

$$CB=\frac{1}{\varepsilon_0(\varepsilon_c+\frac{1}{2}\sum_{q=1}^{Q}c_{0,q})+\frac{\sigma\Delta t}{2}}, \quad (15b)$$

$$\psi_{\rho,q}^{n+1}=\exp(p_q\Delta t)\cdot\psi_{\rho,q}^{n}+c_{0,q}(E_\rho^n+E_\rho^n)/2. \quad (16)$$

Similarly, we can derive the updating equation for E_z:

$$\begin{aligned} E_{z\,i,j+1/2}^{n+1} &= CA\cdot E_{z\,i,j+1/2}^{n} \\ &+CB\cdot\varepsilon_0\cdot\sum_{q=1}^{Q}\left\{\left[1-\exp(p_q\Delta t)\right]\psi_{z,qi,j+1/2}^{n}\right\} \\ &+CB\cdot\Delta t\cdot\left(\frac{H_{\varphi\,i+1/2,j+1/2}^{n+1/2}-H_{\varphi\,i-1/2,j+1/2}^{n+1/2}}{\Delta\rho}\right. \\ &\left.+\frac{H_{\varphi\,i+1/2,j+1/2}^{n+1/2}+H_{\varphi\,i-1/2,j+1/2}^{n+1/2}}{2\rho_i}\right) \end{aligned}. \quad (17)$$

CA, CB are the same as (15). Since (1a) has none dispersive parameters, the updating equation for H_φ is:

$$\begin{aligned} H_\varphi^{n+1/2}(i+1/2,j+1/2) &= H_\varphi^{n-1/2}(i+1/2,j+1/2) \\ -CC\cdot&\left[\frac{E_\rho^n(i+1/2,j+1)-E_\rho^n(i+1/2,j)}{\Delta z}\right. \\ &\left.-\frac{E_z^n(i+1,j+1/2)-E_z^n(i,j+1/2)}{\Delta\rho}\right] \end{aligned}, \quad (18)$$

where $CC=\Delta t/\mu_0$.

(14), (17) and (18) are the updating equations for the dispersive soil.

D. CPML for the dispersive soil

The absorbing boundary condition is an essential technique in truncating the FDTD computational domain for open problem simulations. The Mur's boundary [16] is commonly employed in the FDTD simulations of LEMP [3, 5]. However, the absorbing performance of the Mur's boundary degrades severely when terminates the dispersive medium. The complex frequency-shifted PML (CFS-PML) has been proven to be very efficient for truncating the dispersive medium [17]. The modified Maxwell's scalar equations in CPML can be obtained from the stretched cylindrical coordinate (TMz) [18]:

$$-\mu_0\frac{\partial H_\varphi}{\partial t}=\frac{1}{s_z}\frac{\partial E_\rho}{\partial z}-\frac{1}{s_\rho}\frac{\partial E_z}{\partial\rho}, \quad (19a)$$

$$\frac{\partial D_z}{\partial t}+\sigma E_z=\frac{1}{s_\rho}\frac{\partial(H_\varphi)}{\partial\rho}+\frac{1}{s_\varphi}\frac{H_\varphi}{\rho}, \quad (19b)$$

$$-\frac{\partial D_\rho}{\partial t}-\sigma E_\rho=\frac{1}{s_z}\frac{\partial H_\varphi}{\partial z}, \tag{19c}$$

where

$$s_\rho=k_\rho+\sigma_\rho/(\alpha_\rho+j\omega\varepsilon_0), \tag{20a}$$

$$s_z=k_z+\sigma_z/(\alpha_z+j\omega\varepsilon_0), \tag{20b}$$

$$\begin{aligned}s_\varphi&=k_\varphi+\sigma_\varphi/\alpha_\varphi+j\omega\varepsilon_0\\&=(1/\rho)[\rho_0+\int_{\rho_0}^{\rho}(k_\rho+\sigma_\rho/(\alpha_\rho+j\omega\varepsilon_0))d\rho'],\end{aligned} \tag{21}$$

ρ_0 represents the interface between FDTD and PML grids. Based on the semi-analytical recursive convolution (SARC) algorithm [11], the CPML equations for truncating the dispersive soil can be derived as:

$$\begin{aligned}&E_\rho^{n+1}{}_{i+1/2,j}=CA\cdot E^n_{\rho i+1/2,j}\\&-CB\cdot\Delta t\cdot\left(\frac{H_\varphi^{n+1/2}{}_{i+1/2,j+1/2}-H_\varphi^{n+1/2}{}_{i+1/2,j-1/2}}{k_z\Delta z}+\phi^{n+1/2}_{e\rho z\ i+1/2,j}\right),\\&+CB\cdot\varepsilon_0\cdot\sum_{q=1}^{Q}((1-\exp(p_q\Delta t))\psi^n_{\rho,qi+1/2,j})\end{aligned} \tag{22}$$

$$\begin{aligned}&E_z^{n+1}{}_{i,j+1/2}=CA\cdot E^n_{z\,i,j+1/2}\\&+CB\cdot\varepsilon_0\cdot\sum_{q=1}^{Q}\left\{\left[1-\exp(p_q\Delta t)\right]\psi^n_{z,qi,j+1/2}\right\}\\&+CB\cdot\Delta t\cdot\left(\begin{array}{l}\dfrac{H_\varphi^{n+1/2}{}_{i+1/2,j+1/2}-H_\varphi^{n+1/2}{}_{i-1/2,j+1/2}}{k_\rho\Delta\rho}+\phi^{n+1/2}_{ez\rho\ i,j+1/2}\\+\dfrac{H_\varphi^{n+1/2}{}_{i+1/2,j+1/2}+H_\varphi^{n+1/2}{}_{i-1/2,j+1/2}}{k_\varphi 2\rho_i}+\phi^{n+1/2}_{ez\varphi\ i,j+1/2}\end{array}\right),\end{aligned} \tag{23}$$

$$\begin{aligned}&H_\varphi^{n+1/2}{}_{i+1/2,j+1/2}=H_\varphi^{n-1/2}{}_{i+1/2,j+1/2}\\&-CC\cdot\left[\begin{array}{l}\dfrac{E^n_{\rho i+1/2,j+1}-E^n_{\rho i+1/2,j}}{k_z\Delta z}+\phi^n_{h\varphi z i+1/2,j+1/2}\\-\dfrac{E^n_{z\,i+1,j+1/2}-E^n_{z\,i,j+1/2}}{k_\rho\Delta\rho}-\phi^n_{h\varphi\rho i+1/2,j+1/2}\end{array}\right],\end{aligned} \tag{24}$$

The auxiliary variables ϕ for E are updated by:

$$\begin{aligned}\phi^{n+1/2}_{e\rho z\ i+1/2,j}&=b_z\cdot\phi^{n-1/2}_{e\rho z\ i+1/2,j}\\&+a_z\cdot\frac{H_\varphi^{n+1/2}{}_{i+1/2,j+1/2}-H_\varphi^{n+1/2}{}_{i+1/2,j-1/2}}{\Delta z},\end{aligned} \tag{25a}$$

$$\begin{aligned}\phi^{n+1/2}_{ez\rho\ i,j+1/2}&=b_\rho\cdot\phi^{n-1/2}_{ez\rho\ i,j+1/2}\\&+a_\rho\cdot\frac{H_\varphi^{n+1/2}{}_{i+1/2,j+1/2}-H_\varphi^{n+1/2}{}_{i-1/2,j+1/2}}{\Delta\rho},\end{aligned} \tag{25b}$$

$$\begin{aligned}\phi^{n+1/2}_{ez\varphi\ i,j+1/2}&=b_\varphi\cdot\phi^{n-1/2}_{ez\varphi\ i,j+1/2}\\&+a_\varphi\cdot\frac{H_\varphi^{n+1/2}{}_{i+1/2,j+1/2}+H_\varphi^{n+1/2}{}_{i-1/2,j+1/2}}{2\rho_i},\end{aligned} \tag{25c}$$

where $b_i=e^{(-(\sigma_i/k_i+\alpha_i)(\Delta t/\varepsilon_0))}$, $a_i=(\sigma_i/k_i^2\alpha_i+\sigma_i k_i)(b_i-1)$, $i=\rho,z,\varphi$. The updating equations for $\phi_{h\varphi z}$, $\phi_{h\varphi\rho}$ can be derived similarly, which has the same form as (25a) and (25b).

III. NUMERICAL RESULTS AND DISCUSSIONS

A. Performance of the CPML

We first simulate a point source radiation using both the proposed CPML boundary and Mur's absorbing boundary. The simulation configuration is shown in Fig. 4 (a). The overall computation domain is defined by 50*50 cells with ten-cell-thick CPML. The source located at grid point (0, 26) is given by $H_\varphi(t)=-2(\frac{t-t_0}{t_w})\exp(-(\frac{t-t_0}{t_w})^2)$ with $t_w=50\Delta t$, $t_0=200\Delta t$. The observation point is placed next to the PML boundary at grid point (12, 38). The relative reflection error is calculated as follows:

$$\text{Error}=20\log_{10}(|H_\varphi(t)-H_\varphi^{ref}(t)|/|H_{\varphi\,\max}^{ref}(t)|), \tag{26}$$

where the H_φ^{ref} is the reference result from an extended simulation with no reflection coming from the boundary.

Figure 4 (b) shows the comparison of reflection errors from CPML and Mur's boundary. It can be observed that the CPML shows excellent absorbing performance, which is much better than the Mur's boundary.

B. Evaluation of the LEMP

In this study, the modified transmission line with linear current decay with height (MTLL) [19] is adopted for modeling the lightning return stroke channel with H=7500m, assuming a return stroke speed v=1.3e8m/s. The channel height is 2000m and the channel base current is represented by Heidler's function [20]:

$$\begin{aligned}i(0,t)=\frac{I_{01}}{\eta}\cdot\frac{(t/\tau_1)^2}{(t/\tau_1)^2+1}\cdot\exp(-t/\tau_2)\\+I_{02}\left[\exp(-t/\tau_3)-\exp(-t/\tau_4)\right]\end{aligned}, \tag{27}$$

with parameters listed in Table 2.

Table 2: Parameters of the channel base current

I_{01}/kA	I_{02}/kA	τ_1/μs	τ_2/μs	τ_3/μs	τ_4/μs	η
9.9	7.5	0.072	5.0	100.0	6.0	0.845

The parameters of the dispersive soil are obtained from the LS model with the water content of 1.65, which is associated with the low-frequency conductivity of σ_0=0.0005 S/m. Calculations are carried out by the proposed FDTD method with frequency-dependent

soil parameters (FD-FDTD) and the traditional FDTD method with constant soil parameters (CP-FDTD, σ =0.0005 S/m, ε_r =10). For comparison, the LEMP is also evaluated by the Cooray–Rubinstein (CR) formulation with frequency-dependent soil parameters.

The horizontal electric fields evaluated by different methods are shown in Fig. 5. As we can see, the results of FD-FDTD method agree well with the CR approximation, which prove that the proposed FDTD method can evaluated the LEMP with dispersive soil efficiently. On the other hand, the results of CP-FDTD display obvious deviations from the CR approximations, which validate the necessity to consider the dispersive property of soil in the evaluation of LEMP.

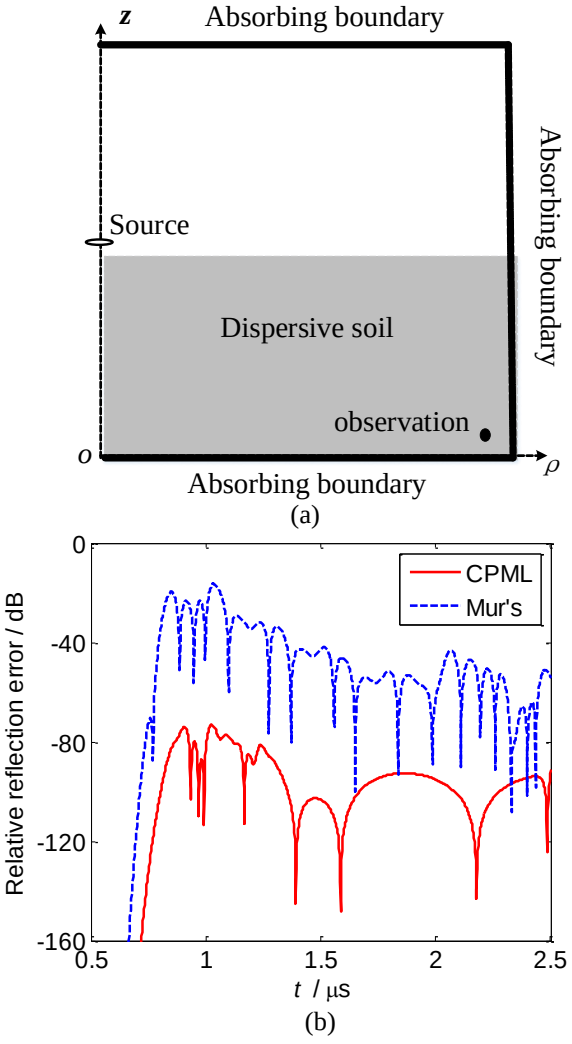

Fig. 4. Comparison of the absorbing performances of CPML and Mur's boundary: (a) computational configurations and (b) relative reflection errors.

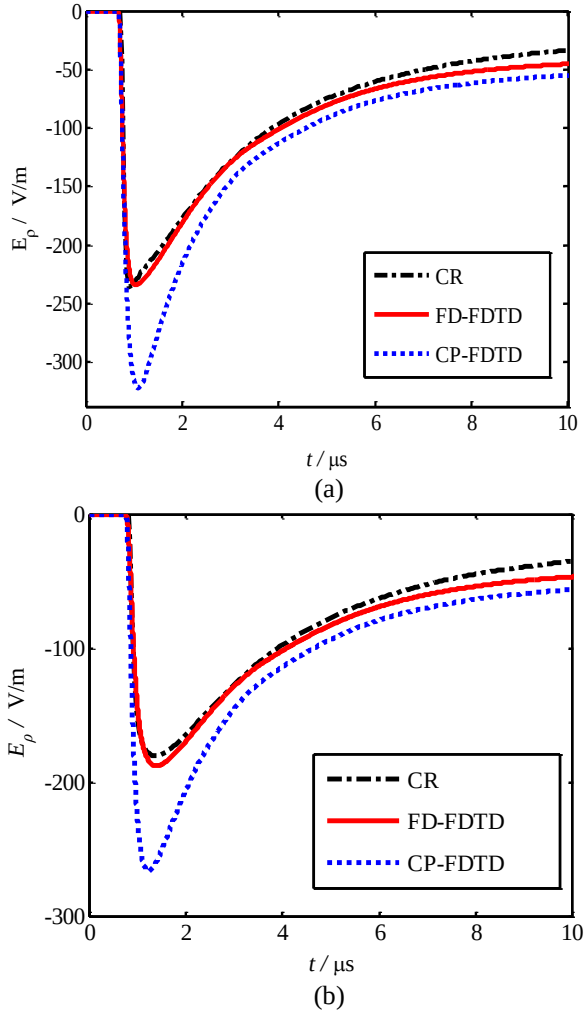

Fig. 5. The horizontal electric fields evaluated by different methods at 200m away from the lightning channel: (a) 1m below the ground and (b) 10m below the ground.

C. Effects of the soil dispersion

In order to further investigate the effect of soil dispersion, we evaluate the LEMPs with different water content percentage of p=1.65%, 5.3% and 11.6%, which are respectively associated with low-frequency conductivities of σ=0.0005, 0.003, and 0.01 S/m [6]. As comparisons, simulations of the traditional FDTD method with constant soil parameters are carried out simultaneously, with ε_r =10, σ=0.0005, 0.003 and 0.01 S/m respectively.

The horizontal electric fields calculated by the two methods with different soil water contents are shown in Fig. 6. It is shown that the dispersive property of the soil results in an attenuation of the amplitude of the

horizontal electric fields. As the decrease of the water content, the decrease of the amplitude becomes more noticeable. Therefore, the dispersive property of the soil should not be neglected in the evaluation of LEMP, especially for the poorly conducting soil.

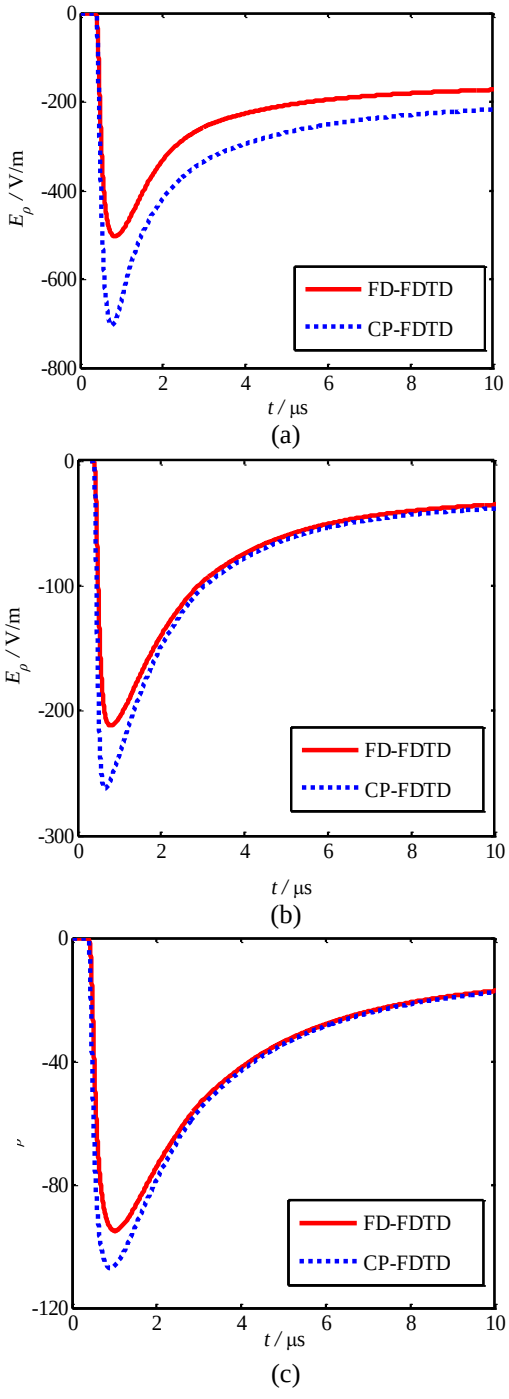

Fig. 6. The horizontal electric fields evaluated with different soil water contents (100m away from the lightning channel, 5m below the ground): (a) p=1.65, (b) p=5.3, and (c) p=11.6.

IV. CONCLUSION

To precisely evaluate the LEMP, the 2D-FDTD method in cylindrical coordinates is further developed for simulating the dispersive soil, by employing the SARC scheme. The cylindrical CPML is also derived for truncating the dispersive soil. The numerical results validate that the proposed method can evaluate the LEMP efficiently with the soil dispersion considered, which leads to a more accurate results than the FDTD methods that disregard the soil dispersion. It was also shown that the soil dispersion can significantly affect the LEMP values for soils with very low conductivity. The proposed method inherits the advantages of the FDTD method, which is efficient in modeling the inhomogeneous ground and the rough ground surface. The proposed method provides an efficient way to an accurate evaluation of LEMP with FDTD, which can be further incorporated into the simulations of more complicated LEMP problems.

ACKNOWLEDGMENT

This work was supported by NSFC in China under Grant No. 51477183 and Jiangsu Natural Science Foundation No. BK20170757.

REFERENCES

[1] M. Paolone, F. Rachidi, A. Borghetti, et al., "Lightning electromagnetic field coupling to overhead lines: Theory, numerical simulations, and experimental validation," *IEEE Trans. Electromagn. Compat.*, vol. 51, no. 3, pp. 532-547, 2009.

[2] M. Albani, A. Mazzinghi, and A. Freni, "Rigorous MoM analysis of finite conductivity effects in RLSA antennas," *IEEE Trans. Antennas Propagat.*, vol. 59, no. 11, pp. 4023-4032, 2011.

[3] C. Yang and B. Zhou, "Calculation method of electromagnetic field very close to lightning," *IEEE Trans. Electromagn. Compat.*, vol. 49, no. 1, pp. 133-141, 2004.

[4] Y. Baba and V. A. Rakov, "Voltages induced on an overhead wire by lightning strikes to a nearby tall grounded object," *IEEE Trans. Electromagn. Compat.*, vol. 48, no. 1, pp. 212-224, 2006.

[5] B. Yang, B. Zhou, C. Gao, et al., "Using a two-step finite-difference time-domain method to analyze lightning induced voltages on transmission lines," *IEEE Trans. Electromagn. Compat.*, vol. 53, no. 1, pp. 256-260, 2011.

[6] M. Akbari, K. Sheshyekani, A. Pirayesh, et al., "Evaluation of lightning electromagnetic fields soil electrical parameters and their induced voltages on overhead lines considering the frequency dependence," *IEEE Trans. Electromagn. Compat.*, vol. 55, no. 6, pp. 1210-1219, 2013.

[7] J. Paknahad, K. Sheshyekani, F. Rachidi, et al., "Evaluation of lightning-induced currents on

cables buried in a lossy dispersive ground," *IEEE Trans. Electromagn. Compat.*, vol. 56, no. 6, pp. 1522-1529, 2014.

[8] P. B. Johns and R. B. Beurle, "Numerical solutions of 2-dimensional scattering problems using a transmission-line matrix," *Proc. IEE*, vol. 118, no. 9, pp. 1203-1208, 1971.

[9] A. Ruehli, "Equivalent circuit models for three-dimensional multiconductor systems," *IEEE Trans. Microw. Theory Techn.*, vol. 22, no. 3, pp. 216-221, 1974.

[10] B. Gustavsen and A. Semlyen, "Rational approx.-imation of frequency domain responses by vector fitting," *IEEE Transactions on Power Delivery*, vol. 14, no. 3, pp. 1052-1061, 1999.

[11] Y. Q. Zhang and D. B. Ge, "A unified FDTD approach for electromagnetic analysis of dispersive objects," *Progress in Electromagnetics Research*, vol. 96, pp. 155-172, 2009.

[12] V. Cooray, "Some considerations on the 'Cooray–Rubinstein' approximation used in deriving the horizontal electric field over finitely conducting ground," *IEEE Trans. Electromagn. Compat.*, vol. 44, no. 4, pp. 560-565, 2002.

[13] A. Taflove and S. C. Hagness, *Computational Electrodynamics The Finite-Difference Time-Domain Method*, 3rd ed., Norwood, MA: Artech House, 2005.

[14] C. L. Longmire and K. S. Smith, "A universal impedance for soils," *Defense Nuclear Agency*, Topical Report for Period, Santa Barbara, CA, USA, 1975.

[15] D. Cavka, N. Mora, and F. Rachidi, "A comparison of frequency-dependent soil models: Application to the analysis of grounding systems," *IEEE Trans. Electromagn. Compat.*, vol. 48, no. 1, pp. 177-187, 2013.

[16] G. Mur, "Absorbing boundary conditions for the finite-difference approximation of the time-domain electromagnetic field equations," *IEEE Trans. Electromagn. Compat.*, vol. 23, pp. 377-382, 1981.

[17] J. A. Roden and S. D. Gedney, "Convolution PML (CPML): An efficient FDTD implementation of the CFS-PML for arbitrary media," *Microw. Opt. Tech. Lett.*, vol. 27, no. 5, pp. 334-339, 2000.

[18] J. Liu, G. Wan, J. Zhang, and X. Xi, "An effective CFS-PML implementation for cylindrical coord-inate FDTD method," *IEEE Microw. Wireless Compon. Lett.*, vol. 22, no. 6, pp. 300-302, 2012.

[19] V. A. Rakov and A. A. Dulzon, "Calculated electromagnetic fields of lightning return stroke," *Tekh. Elektr.*, no. 1, pp. 87-89, 1987.

[20] F. Heidler, "Travelling current source model for LEMP calculation," *Proc. 6th Int. Symp. Electromagn. Compat.*, Zurich, Switzerland, pp. 157-162, 1985.

Zheng Sun received the B.S. degree in Automatic Control in 2009 from Sourthest University, Jiangsu, China and Ph.D. degree of Electrical Engineering in PLA University of Science & Technology, Jiangsu, China, in 2014, respectively. He is currently working as a Lecturer in the PLA Army Engineering University, with his main interests on computing electromagnetics and lightning protections.

LiHua Shi received the B.S. degree from Xidian University, Shanxi, China, in 1990, the M.S. degree from Nanjing Engineering Institute, Jiangsu, China, in 1993,and the Ph.D. degree from the Nanjing University of Aeronautics and Astronautics, Jiangsu, in 1996,respectively. During 2001, he worked as a Visiting Scholar in Stanford University. He is currently working as a Professor in the PLA Army Engineering University, with his main interests on time-domain measurement technology.

Shi is a Member of the IEEE's I&M society and EMC society.